Supplementary Materials and Methods

Cell culture and transfection. Mouse embryonic fibroblasts (MEFs) were derived from the embryos produced by crossing heterozygotes (+/-) (pure C57Bl/6j background, (1, 2)) in the context of a project approved by the ‘‘Comité d’Ethique pour l’expérimentation animale Charles Darwin’’ (Ce5/2009/052). They were obtained on embryonic day 14.5, as previously described (3), and were cultured in DMEM supplemented with 10% fetal bovine serum (Gibco), 1% L-glutamine and 1% penicillin-streptomycin.

Confocal microscopy. MEFs were incubated for 30 minutes with 500 nM ER-tracker DPX and 200 nM MitoTracker Red. Blue diode (405 nm) and HeNe (543 nm) laser lines were used for excitation. Images were obtained with a 0.5 µm step in the *z*-direction on a Leica SP2 AOBS AOTF confocal microscope equipped with a PlanApo X63 (NA 1.4) numerical aperture objective. Mander’s overlap coefficient was obtained for ER and mitochondrial signals with the Wright Cell Imaging Facility (WCIF) ImageJ plugin, for at least 26 cells from each of five wild-type and five *PARK2* KO MEF lines.

Electron microscopy. The proximity of the ER and mitochondria in MEFs was analyzed by obtaining images such that all mitochondria and their vicinity (less than 2 µm) could be reconstituted in a given cell with the stitching function of Photoshop. Using the segment-drawing function of ImageJ, we then measured the distance between a given mitochondrion and its closest visible ER membrane. When no clear separation between the ER and a mitochondrion could be found, we considered the two organelles to be “in direct contact”. At least 25 cells from each of four wild-type and four *PARK2* KO MEF lines were analyzed.

Generation and characterization of induced pluripotent stem cells (iPSC). iPSC clones generated from Control 9 (p.[Ala291ValfsX8];[=]) and Patient 2 (p.[Ala291ValfsX8];[Arg42Pro]) fibroblasts were obtained by reprogramming fibroblasts by retroviral transduction with the four Yamanaka’s factors OCT-4, SOX2, KLF4 and c-MYC, as previously reported (4), and iPSC clones from Control 2 fibroblasts were generated with the integration-free CytoTune-iPS 2.0 Sendai Reprogramming Kit (Life Technologies). For Control 9 and Patient 2, iPSC clones were individually picked and expanded on feeder layers of mitomycin C-inactivated murine embryonic fibroblast (MEF) cells, in a damp 5% CO_2 incubator at 37°C,

in Knock-Out (KO)-DMEM supplemented with 20% KO Serum Replacement (KSR), 1 mM L-glutamine, 1% non-essential amino acids, 0.1 mM β-mercaptoethanol and 10 ng/ml basic (b) FGF (all from Life Technologies). Cultures were fed daily and manually passaged every 5–7 days, then adapted to feeder-free cultures in E8 medium on Geltrex-coated plates with EDTA-mediated passages. For Control 2, iPSC clones were generated directly under feeder-free conditions, picked and transferred to Geltrex-coated plates and cultured in Essential 6 Medium (Life Technologies) with freshly added bFGF. Colonies were passaged with EDTA, and maintained in Essential 8 Medium (Life Technologies) on Geltrex-coated plates. Sendai virus clearance was checked by Scorecard analysis and immunocytochemistry (data not shown).

Quality control for iPSC was performed as suggested by the International Stem Cell Banking Initiative (5). iPSC were treated with collagenase (Life Technologies) and cultured in suspension for 10 days in Essential 6 medium. The EBs were then harvested and either treated with RNAzol RT (Euromedex) for RNA extraction or plated on Geltrex and cultured in fibroblast medium for another 10 days for immunostaining. iPSC and plated EBs were fixed in 4% paraformaldehyde (Euromedex) for 20 minutes, then incubated overnight at 4°C with primary antibodies in blocking solution (1% bovine serum albumin and 2% normal goat serum in 1X PBS) supplemented with 0.1% Triton-X100. The following primary antibodies were used: monoclonal anti-TRA1-60 and anti-TRA1-81 (Millipore ES Cell Characterization Kit), monoclonal anti-OCT-3/4 (clone C-10, Santa Cruz), polyclonal anti-NANOG (Proteintech), monoclonal anti-MAP2, anti-SMA and anti-AFP (Millipore Human Embryonic Germ Layer Characterization Kit). Secondary antibodies (Life Technologies) were incubated in blocking solution for 1 hour at room temperature before mounting. Images were captured on a Carl Zeiss AxioScope A1 with ZEN acquisition software. To analyze pluripotency and differentiation potential with the TaqMan hPSC Scorecard Panel, RNA extracts from iPSC and EBs were sent to Thermo Fisher Scientific. The expression of a panel of 93 genes from five classes (pluripotent, ectoderm, mesoderm, endoderm and control) was verified and compared with that of a reference set of nine iPS and ES cell clones. Results are expressed as a score relative to the reference set. Genetic integrity was evaluated by R-banded karyotype analysis at

the Genetic Department, Hôpital Pitié-Salpêtrière, Paris, France (data not shown). All iPSC clones showed normal karyotypes (data not shown).

Differentiation of iPSC into dopaminergic neurons. A rosette-based or floor-plate protocol for the differentiation of iPSC into dopaminergic neurons was applied. For the rosette-based approach (6, 7), EBs were plated on Geltrex in DMEM-F12-1% N_2 (Life Technologies) medium, supplemented with 20 ng/ml bFGF. After 3 days, neural rosettes were manually collected and mildly dissociated, prior plating on Poly-D-Lysine coated coverslips or Lab-Tek wells in Neurobasal medium-2% B27 medium (Life Technologies), supplemented with 20 ng/ml BDNF (PeproTech), 10 ng/ml GDNF (PeproTech), 200 μM L-ascorbic acid (Sigma-Aldrich). For the first week, 200 ng/ml mSSH (PeproTech) and 100 ng/ml FGF8 (PeproTech) were added in the medium to induce patterning. We left the cultures to differentiate for 5 more weeks by renewing half of the medium every 3-4 days. For the floor-plate protocol (8, 9), iPSC were plated as single cells on Geltrex-coated plates and progressively exposed to 10 μM SB431542 (Tocris) and 500 ng/ml Noggin (PeproTech) for neural induction, and 200 ng/mSSH , 100 ng/ml FGF8 and 3 μM CHIR99021 (Stemgent) for patterning. After the passaging of neural precursors with Accutase on day 20, further maturation of the cultures was accomplished in poly-L-ornithine/laminin-coated coverslips or Lab-Tek wells in Neurobasal medium-2% B27 medium , supplemented with 20 ng/ml BDNF, 20 ng/ml GDNF , 200 μM L-ascorbic acid, 0.5 mM dibutyryl cAMP (Sigma-Aldrich) and 2 ng/ml TGF-β3 (Sigma-Aldrich). The percentage of neurons and tyrosine hydroxylase (TH)-positive cells in the differentiating cultures was estimated by determining immunofluorescence with polyclonal anti-neuronal class III β-tubulin (TUJ1, Covance) and monoclonal anti-TH (clone LNC1, Millipore) antibodies, followed by imaging and analysis on an ArrayScan XTI HCA Reader.

Patch electrophysiology of iPSC-derived neurons. Currents and membrane potentials from human iPSC-derived cells were recorded with the whole-cell configuration of the patch-clamp technique (10). The Petri dish was transferred to the recording chamber mounted on the stage of an Eclipse-T*i* inverted microscope (Nikon). Patch electrodes were pulled from 1.5 mm borosilicate glass capillaries on a Zeitz DMZ puller (Germany). The resistance of a typical patch pipette is 2-3 MΩ when filled with the

intracellular solution, containing 10 mM KCl, 130 mM K-gluconate, 2 mM $MgCl_2$, 0.1 mM $CaCl_2$, 4 mM ATP-Mg, 0.3 mM GTP, 10 mM Na Phosphocreatine, 1 mM EGTA, and 10 mM HEPES, adjusted to pH 7.2 with KOH. The extracellular solution contained 140 mM NaCl, 3 mM KCl, 1 mM $MgCl_2$, 2 mM $CaCl_2$, 10 mM glucose and 10 mM HEPES adjusted to pH 7.3 with NaOH. Whole-cell recordings were performed with an Axopatch 200B (Axon Instruments, Molecular Devices, USA). Data were low-pass filtered with an eight-pole Bessel filter at 2 kHz and then digitized at a sampling rate of 10 kHz with a Digidata 1440A Analog/Digital interface. Data were acquired with pClamp10 software. Capacitance transients cancelled out. Series resistance was typically between 5 and 7 MΩ and was compensated by at least 70% for voltage-clamp experiments. Holding potentials were corrected for a calculated liquid junction potential of 15 mV. Only cells with a residual series resistance of less than 7 MΩ, after whole-cell configuration was established, were recorded. Electrophysiological recordings were carried out at room temperature (21-23°C). Data were analyzed off-line with Clampfit (pClamp10 suite) and Origin (Origin Lab Corporation) softwares.

Legends to Supplementary Figures

Figure S1. A. Total extracts of MEFs from wild-type and *PARK2* KO mice were analyzed by western blotting with an anti-Parkin antibody. Actin levels were used as a loading control. **B.** MEFs from wild-type and *PARK2* KO mice were loaded with ER Tracker DPX and MitoTracker Red, and analyzed by live-cell confocal laser microscopy. ER-mitochondria colocalization was estimated by determining Mander's overlap coefficient. **C.** The percentage of mitochondria in direct contact with the ER (*Left*) and the mean distance between the two compartments (*Right*) were measured on electron micrographs of MEFs from wild-type and *PARK2* KO mice. Scale bar: 10 µm. *n* represents the number of independent MEF lines for each genotype. Error bars represent the SEM. $**p<0.01$, $***p<0.001$.

Figure S2. Mean mitochondrial size and the percentage of swollen mitochondria were determined on electron micrographs of MEFs from wild-type and *PARK2* KO mice. Scale bar: 1 µm. *n* represents the number of independent MEF lines for each genotype. Error bars represent the SEM.

Figure S3. Effect of the donor age on ER-mitochondria proximity and Ca^{2+} transfers. Scatter plots of Mander's overlap coefficient (**A**), the % surface area near mitochondria covered by ER (**B**), the BK-induced Fura-2 signal peak (**C**) or the pericam 405 excitation fluorescence (**D**) against the age of the donors at the time of skin biopsy. The calculated correlation coefficients indicate lack of correlation between the two variables.

Figure S4. A. Monitoring of the Fura-2 340/387 nm signal ratio in MEFs from wild-type and *PARK2* KO mice before and after stimulation with bradykinin (BK, *Left*). The BK-induced Fura-2 signal peak was calculated for each cell by subtracting the 340/387 nm ratio at t_0 from the maximal ratio (*Right*). **B.** As in (A) after stimulation with histamine (His) in the presence of thapsigargin (Tg) to prevent Ca^{2+} recapture from the ER. *n* represents the number of independent MEF lines for each genotype. Error bars represent the SEM. $*p<0.05$, $**p<0.01$.

Figure S5. Characterization of iPSC clones. **A.** Representative images of the immunostaining of iPSC clones against a panel of pluripotency markers: OCT-3/4, NANOG, TRA1-60, TRA1-81 and SSEA-4. Nuclei were stained with DAPI. **B.** Representative images of plated EBs immunostained for lineage-

specific markers: MAP2 or TUJ1 for ectoderm, SMA for mesoderm, and AFP or SOX17 for endoderm. **C.** Pluripotency and tri-lineage differentiation potential were verified by the Scorecard analysis of RNA from iPSC and EBs from Control 2. Results are expressed as a score relative to a reference set of standard iPS and ES cell clones. Scale bars: 100 µm.

Figure S6. Molecular and functional characterization of human iPSC-derived neurons. **A.** Immunostaining of iPSC-derived neuronal cultures after 4 weeks of differentiation, with anti-TH and anti-TUJ1 antibodies. Nuclei were labeled with Hoechst 33342. The mean percentage of neuronal cells in the differentiating cultures was 33% (TUJ1- *versus* Hoechst-positive cells), whereas the percentage of TH-positive neuronal cells was 16% (TH- *versus* TUJ1-positive cells). Scale bar: 10 µm. **B.** Whole-cell patch clamp analysis of iPSC-derived neurons at 3 weeks of differentiation. *Top*: Representative voltage-clamp recordings showing fast, inactivating sodium currents and potassium currents in control and patient iPSC-derived neurons. Voltage-dependent currents were elicited from a holding potential of -80 mV by delivering step depolarization ranging from -60mV to +60 mV with a 5-second inter-sweep interval. *Bottom*: Representative current-clamp recordings showing single or repetitive firing observed in response to square current injection in the same control and patient iPSC-derived neurons. A current was injected to hold the membrane potential around -70mV and a series of depolarizing current steps of 10, 40 and 80 pA were applied. The resting membrane potentials for Control 2, Control 9 and Patient 2 iPSC-derived neurons were -61 mV, -65 mV and -65 mV.

Figure S7. A. Mfn2 levels were analyzed by western blotting total extracts of human fibroblasts with *PARK2* mutations (Patients 1-3 and 5-7) and control (Controls 2-6) fibroblasts, with normalization against actin. **B.** As in (A) for wild-type and *PARK2* KO MEFs. **C.** Quality of the subcellular fractions isolated from mouse liver, evaluated by western blot analysis for the MAM-enriched proteins PS2, ACSL4/FACL4, Erlin2 and BiP; the mitochondrial markers PMPCB and cytochrome *c*; and Mfn2. The punctuated line separates western blot analyses of the same subcellular fractions (20µg) loaded on two independent gels. The asterisk (*) indicates the presence of a nonspecific band. *n* represents the number of fibroblast lines used from one experiment representative of two. Error bars represent the SEM.

References

1. Itier, J.M., Ibanez, P., Mena, M.A., Abbas, N., Cohen-Salmon, C., Bohme, G.A., Laville, M., Pratt, J., Corti, O., Pradier, L. *et al.* (2003) Parkin gene inactivation alters behaviour and dopamine neurotransmission in the mouse. *Hum. Mol. Genet.*, **12**, 2277-2291.

2. Damiano, M., Gautier, C.A., Bulteau, A.L., Ferrando-Miguel, R., Gouarne, C., Paoli, M.G., Pruss, R., Auchere, F., L'Hermitte-Stead, C., Bouillaud, F. *et al.* (2014) Tissue- and cell-specific mitochondrial defect in Parkin-deficient mice. *PLoS One*, **9**, e99898.

3. Gautier, C.A., Giaime, E., Caballero, E., Nunez, L., Song, Z., Chan, D., Villalobos, C. and Shen, J. (2012) Regulation of mitochondrial permeability transition pore by PINK1. *Mol. Neurodegener.*, **7**, 22.

4. Mangeot, P.E., Dollet, S., Girard, M., Ciancia, C., Joly, S., Peschanski, M. and Lotteau, V. (2011) Protein transfer into human cells by VSV-G-induced nanovesicles. *Mol. Ther.*, **19**, 1656-1666.

5. International Stem Cell Banking, I. (2009) Consensus guidance for banking and supply of human embryonic stem cell lines for research purposes. *Stem Cell Rev*, **5**, 301-314.

6. Lee, S.H., Lumelsky, N., Studer, L., Auerbach, J.M. and McKay, R.D. (2000) Efficient generation of midbrain and hindbrain neurons from mouse embryonic stem cells. *Nat. Biotechnol.*, **18**, 675-679.

7. Yang, D., Zhang, Z.J., Oldenburg, M., Ayala, M. and Zhang, S.C. (2008) Human embryonic stem cell-derived dopaminergic neurons reverse functional deficit in parkinsonian rats. *Stem Cells*, **26**, 55-63.

8. Kriks, S., Shim, J.W., Piao, J., Ganat, Y.M., Wakeman, D.R., Xie, Z., Carrillo-Reid, L., Auyeung, G., Antonacci, C., Buch, A. *et al.* (2011) Dopamine neurons derived from human ES cells efficiently engraft in animal models of Parkinson's disease. *Nature*, **480**, 547-551.

9. Sundberg, M., Bogetofte, H., Lawson, T., Jansson, J., Smith, G., Astradsson, A., Moore, M., Osborn, T., Cooper, O., Spealman, R. *et al.* (2013) Improved cell therapy protocols for Parkinson's disease based on differentiation efficiency and safety of hESC-, hiPSC-, and non-human primate iPSC-derived dopaminergic neurons. *Stem Cells*, **31**, 1548-1562.

10. Hamill, O.P., Marty, A., Neher, E., Sakmann, B. and Sigworth, F.J. (1981) Improved patch-clamp techniques for high-resolution current recording from cells and cell-free membrane patches. *Pflugers Arch.*, **391**, 85-100.

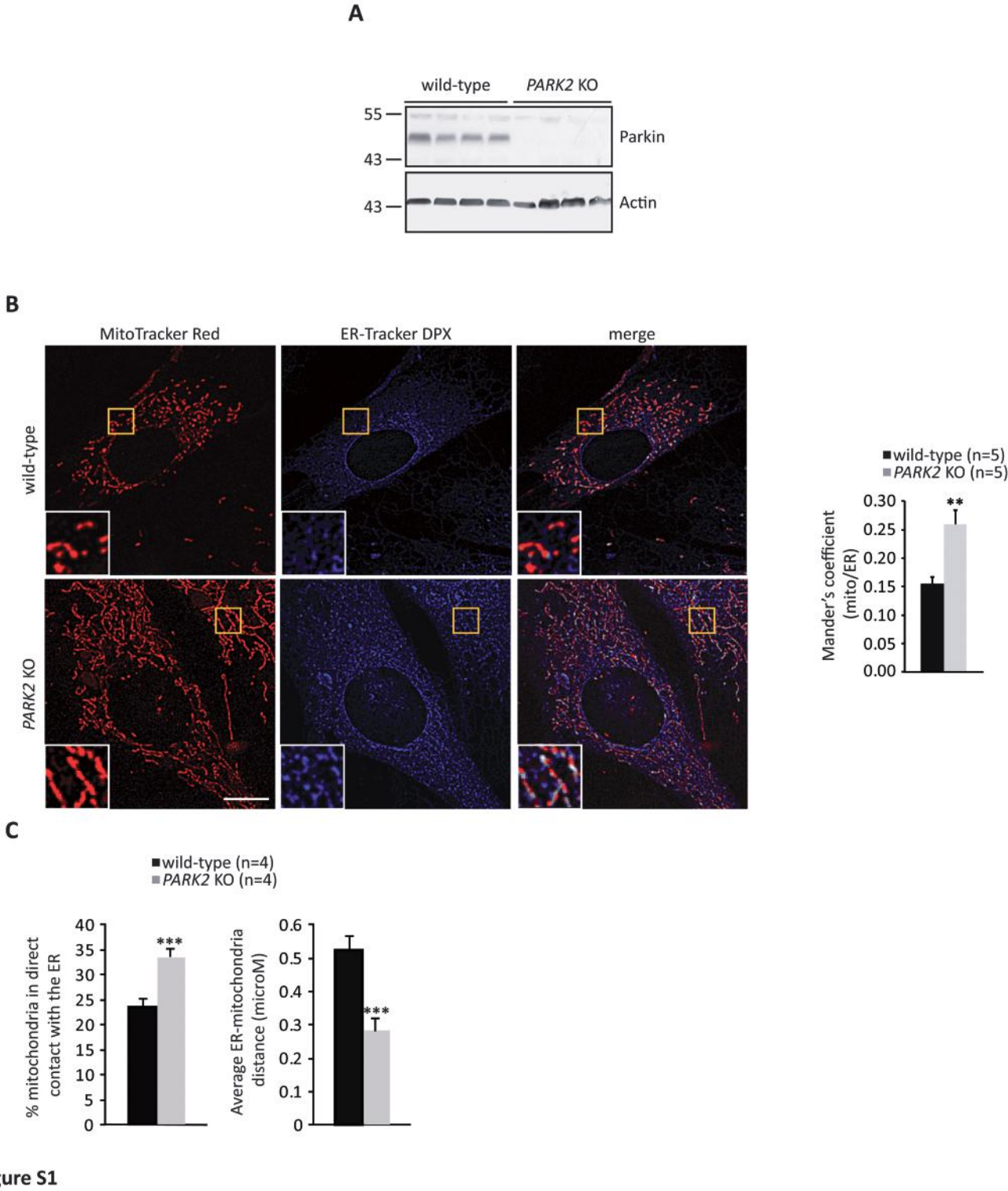
A
wild-type
PARK2 KO
55
43
Parkin
43
Actin
B
MitoTracker Red
ER-Tracker DPX
merge
wild-type
PARK2 KO
wild-type (n=5)
PARK2 KO (n=5)
Mander's coefficient (mito/ER)
0.30
0.25
0.20
0.15
0.10
0.05
0.00
**
C
wild-type (n=4)
PARK2 KO (n=4)
% mitochondria in direct contact with the ER
40
35
30
25
20
15
10
5
0
***
Average ER-mitochondria distance (microM)
0.6
0.5
0.4
0.3
0.2
0.1
0
***

Figure S1

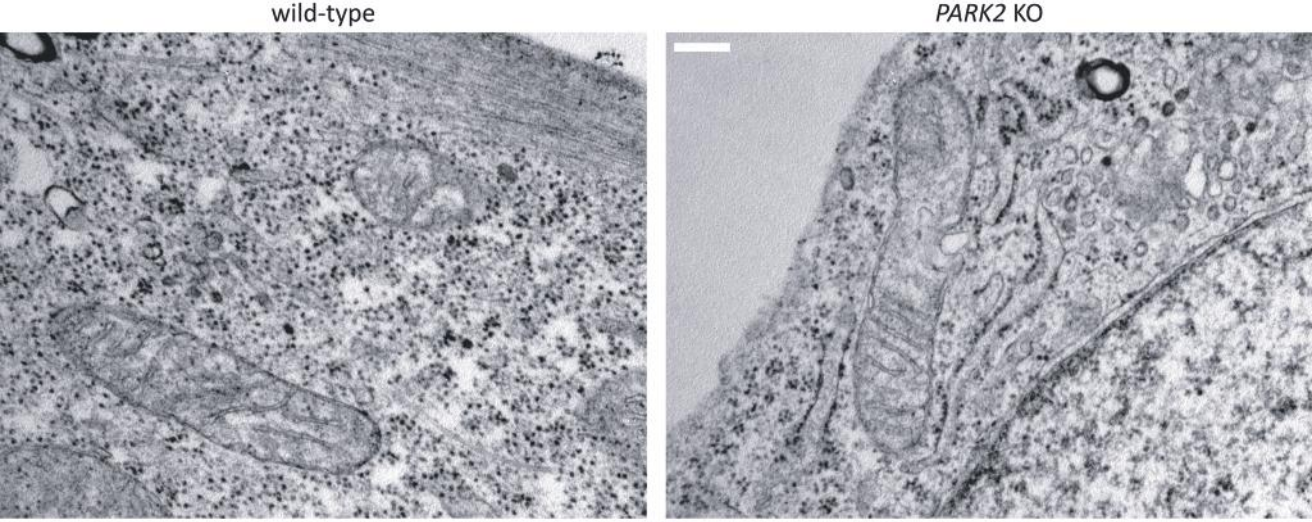
wild-type
PARK2 KO

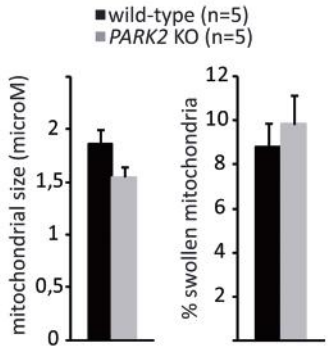
wild-type (n=5)
PARK2 KO (n=5)
mitochondrial size (microM)
2
1,5
1
0,5
0
% swollen mitochondria
12
10
8
6
4
2

Figure S2

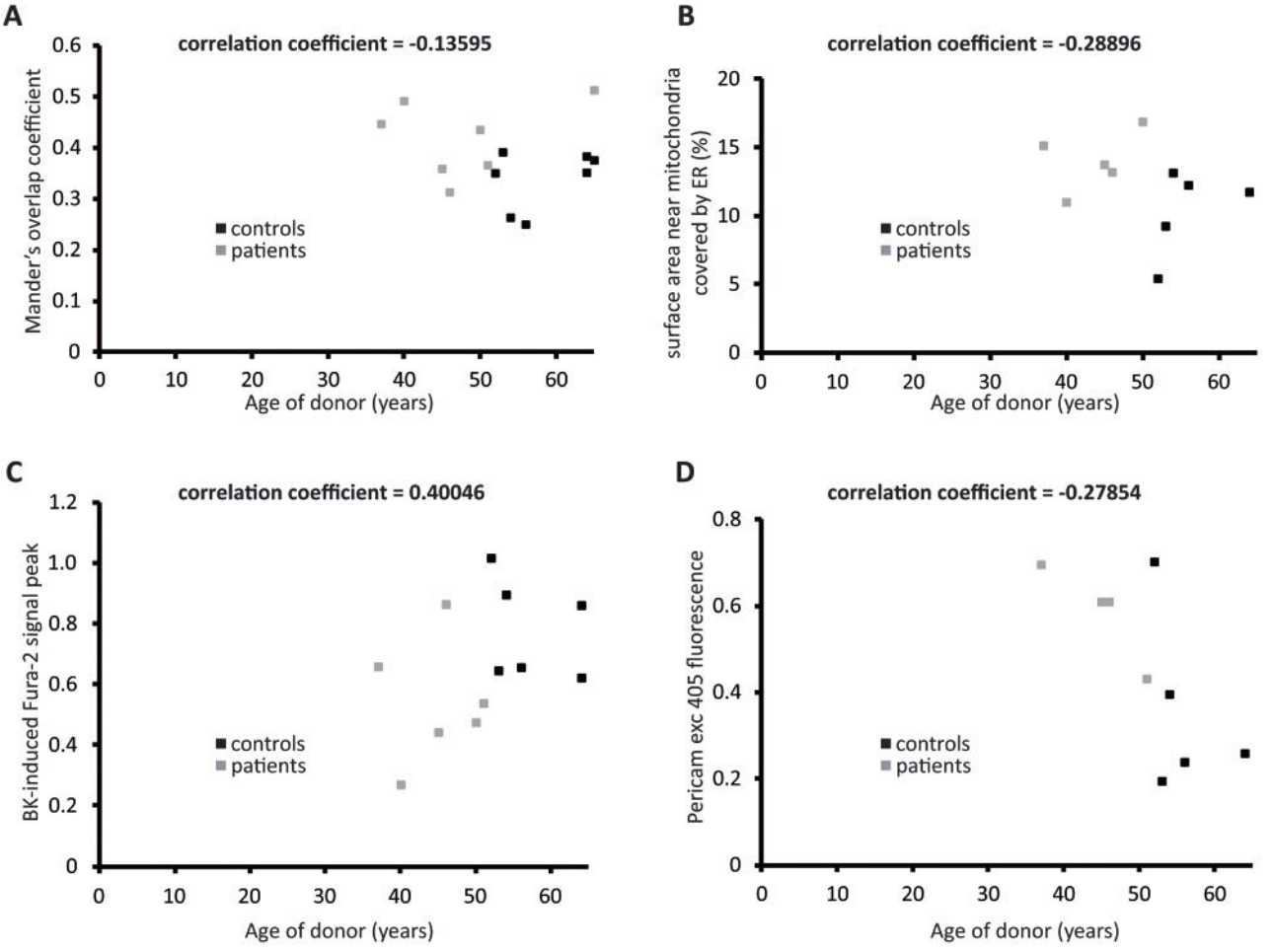
A
correlation coefficient = -0.13595
Mander's overlap coefficient
0.6
0.5
0.4
0.3
0.2
0.1
0
controls
patients
0
10
20
30
40
50
60
Age of donor (years)
B
correlation coefficient = -0.28896
surface area near mitochondria covered by ER (%)
20
15
10
5
0
controls
patients
0
10
20
30
40
50
60
Age of donor (years)
C
correlation coefficient = 0.40046
BK-induced Fura-2 signal peak
1.2
1.0
0.8
0.6
0.4
0.2
0
controls
patients
0
10
20
30
40
50
60
Age of donor (years)
D
correlation coefficient = -0.27854
Pericam exc 405 fluorescence
0.8
0.6
0.4
0.2
0
controls
patients
0
10
20
30
40
50
60
Age of donor (years)

Figure S3

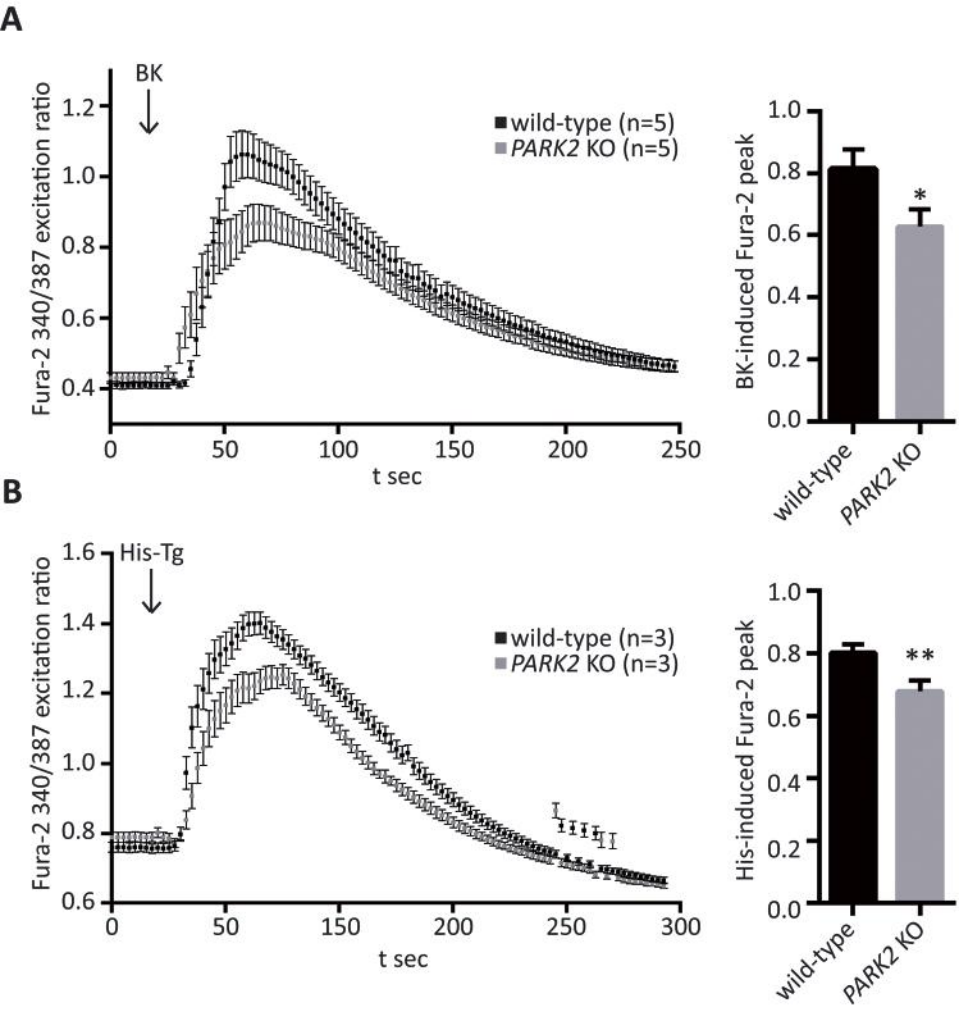
A
BK
wild-type (n=5)
PARK2 KO (n=5)
Fura-2 340/387 excitation ratio
t sec
BK-induced Fura-2 peak
wild-type
PARK2 KO
*
B
His-Tg
wild-type (n=3)
PARK2 KO (n=3)
Fura-2 340/387 excitation ratio
t sec
His-induced Fura-2 peak
wild-type
PARK2 KO
**

Figure S4

A

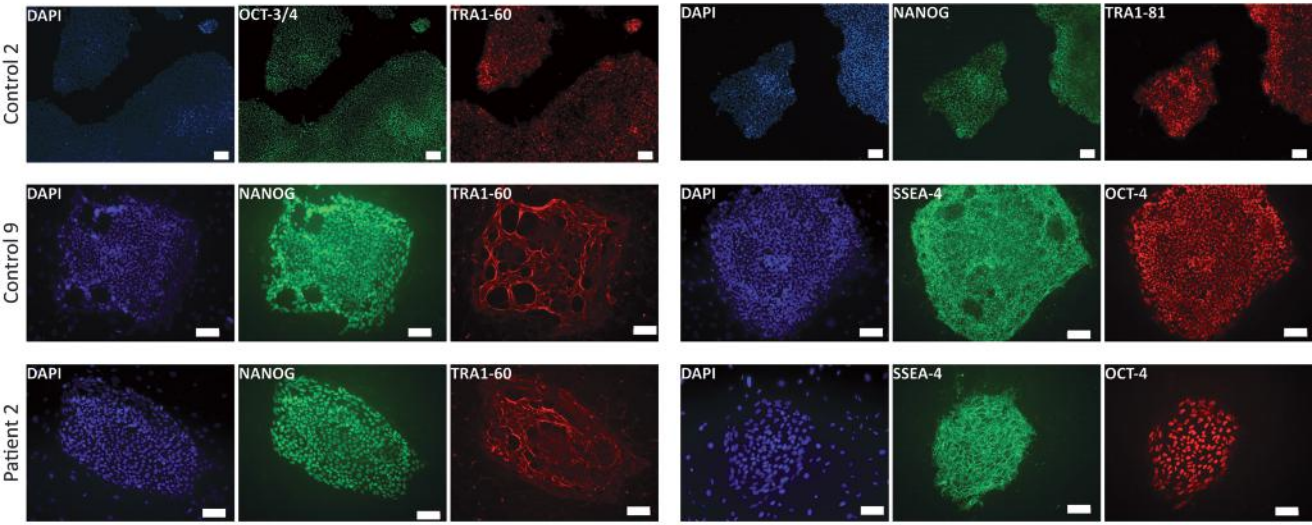

B

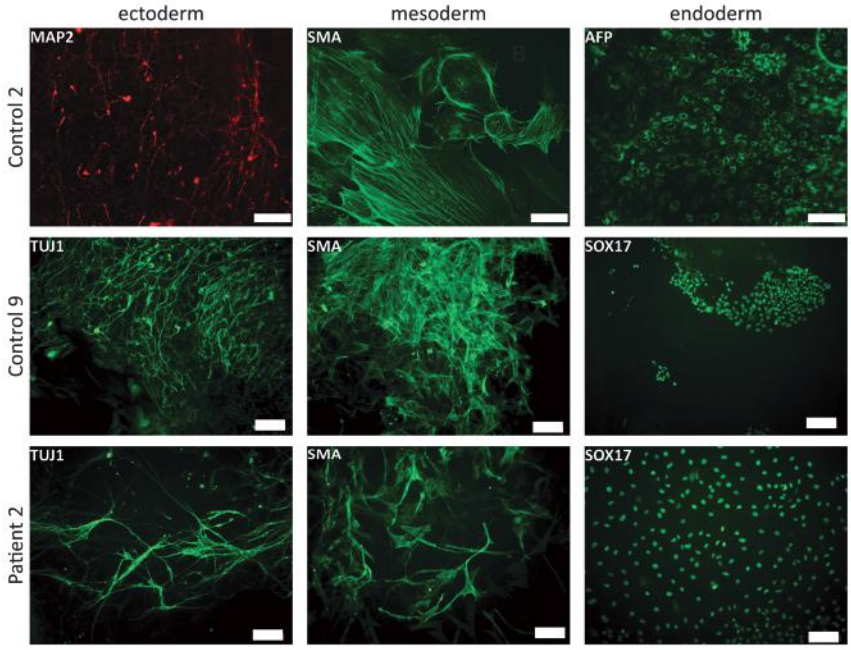

C

Sample Name	Self-renewal	Ectoderm	Mesoderm	Endoderm
iPSc control 2	0,02	-0,09	-1,04	-1,34
EB control 2	-2,58	1,45	0,86	0,65

Gene expression relative to the reference standard

x>1.5	Upregulated
1.0<x<=1.5	
0.5<x<=1.0	
-0.5<=x<=0.5	Comparable
-1.0<=x<-0.5	
-1.5<=x<-1.0	
x<-1.5	Downregulated

Figure S5

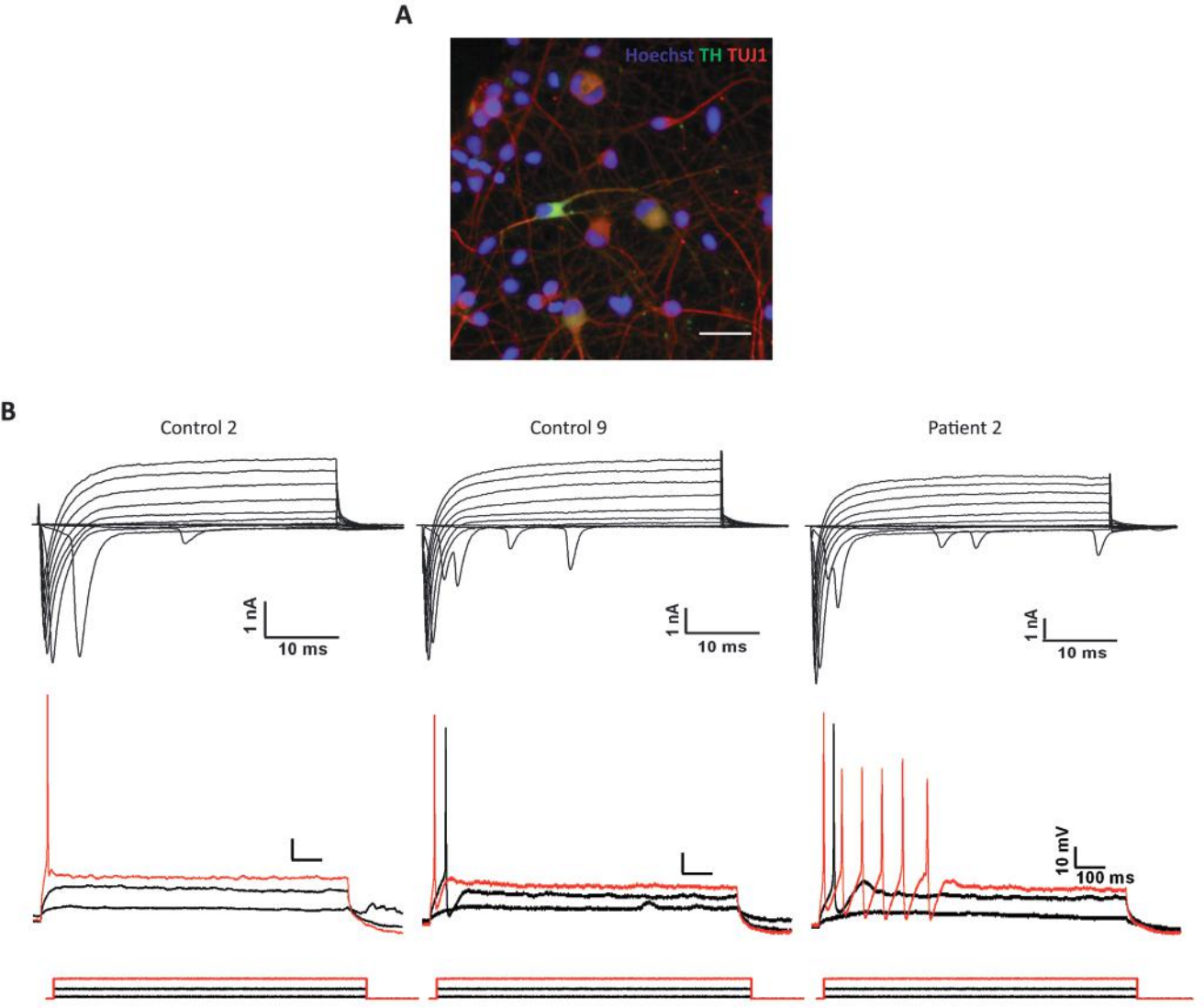
A
Hoechst TH TUJ1
B
Control 2
Control 9
Patient 2
1 nA
10 ms
1 nA
10 ms
1 nA
10 ms
10 mV
100 ms

Figure S6

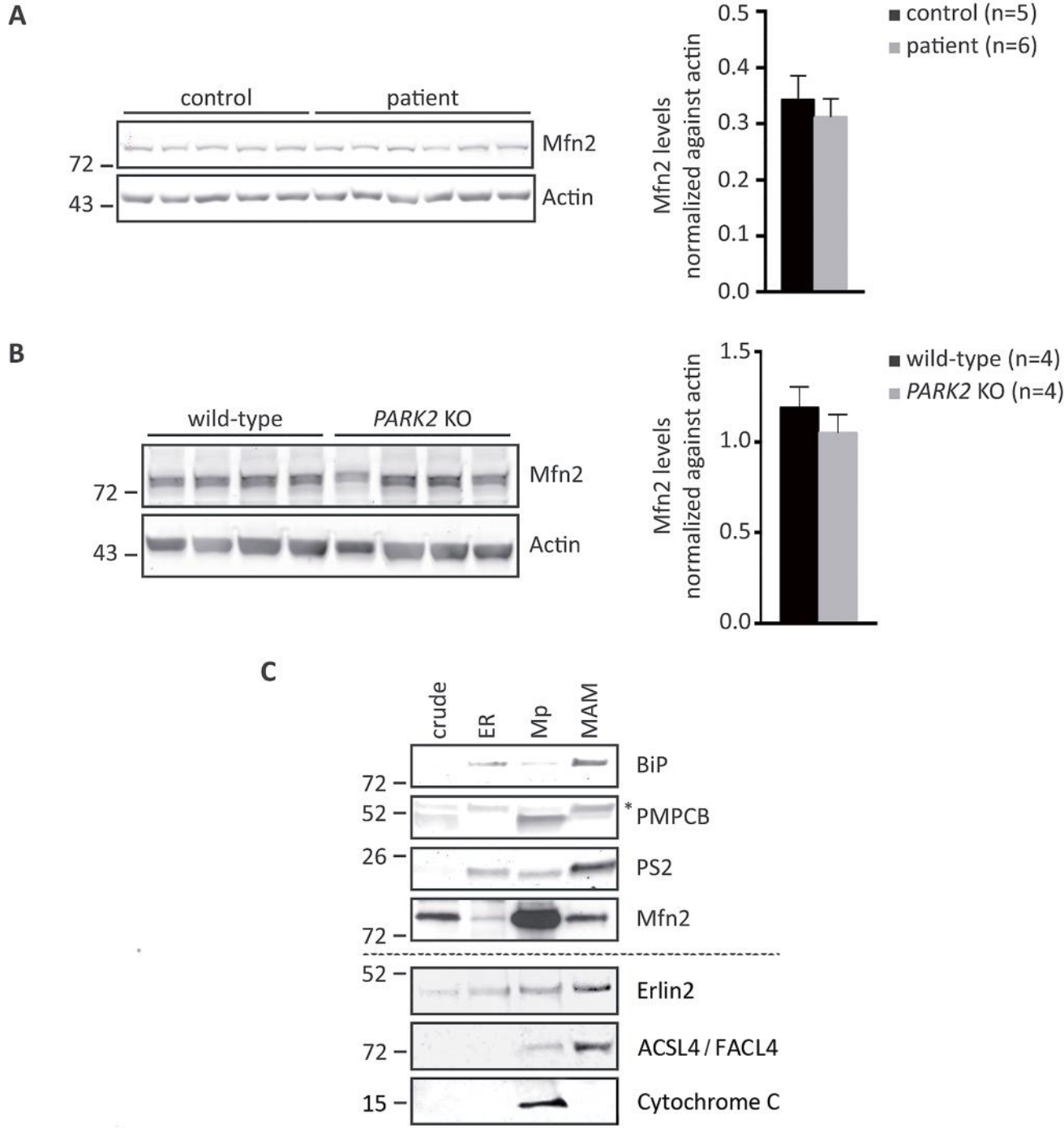
A
control
patient
72
43
Mfn2
Actin
Mfn2 levels normalized against actin
0.5
0.4
0.3
0.2
0.1
0.0
control (n=5)
patient (n=6)
B
wild-type
PARK2 KO
72
43
Mfn2
Actin
Mfn2 levels normalized against actin
1.5
1.0
0.5
0.0
wild-type (n=4)
PARK2 KO (n=4)
C
crude
ER
Mp
MAM
72
52
26
72
52
72
15
BiP
*PMPCB
PS2
Mfn2
Erlin2
ACSL4 / FACL4
Cytochrome C

Figure S7